MESOSCOPIC SPINTRONICS: FLUCTUATION AND LOCALIZATION EFFECTS IN SPIN-POLARIZED QUANTUM TRANSPORT

BRANISLAV K. NIKOLIĆ AND J. K. FREERICKS

Department of Physics, Georgetown University, Washington, DC 20057-0995, U.S.A.
E-mail: bnikolic@physics.georgetown.edu, Web: http://physics.georgetown.edu/∼bnikolic

Using a generalized Landauer-type formula in terms of real⊗spin-space Green functions, we analyze spin-polarized transport in two-dimensional fully quantum-coherent systems by computing components of their exact two-probe zero-temperature conductance matrix, as well as their mesoscopic fluctuations. We find that the interplay of strong Rashba spin-orbit coupling and phase-coherent propagation through disordered *mesoscopic spintronic* devices leads to a dramatic reduction of localization effects on the conductances and their variances. The transport properties also depend on the chosen axis of spin-polarization.

1 Introduction

The orientation of electron spin can survive various forces in metals or semiconductors for long enough time to allow for envisioned quantum technologies that manipulate spin, such as spintronics[1,2] or solid-state quantum computing with spin-based qubits.[3] Recent experimental advances in spintronics have provided an impetus to study spin-polarized transport in two-dimensional electron systems attached to two ferromagnetic contacts. Although many applications require devices operating at room temperature, it is also intriguing to explore quantum interference effects involving both the charge and spin of the electrons in nanoscale samples at very low temperatures $\lesssim$ 1K—a playground of mesoscopic physics over the past two decades.[4] Thus, recent theoretical efforts of the transport community have been moving from *semiclassical* to *quantum* spintronics by extending standard mesoscopic techniques (like the Landauer-Büttiker scattering approach to quantum transport of spin-degenerate particles in finite-size systems[4]) to treat phase-coherent spin-polarized transport in the presence of spin-dependent interactions.[5,6] A particularly important interaction for spintronics is the Rashba type of spin-orbit (SO) coupling,[7] which is different from the more familiar impurity induced and position dependent one in metals.[8] It arises from the asymmetry along the z-axis of the confining quantum well electric potential (generating a magnetic field in the electron rest frame) that creates a two-dimensional (2D) electron gas (xy-plane) on a narrow-gap semiconductor surface. Since the Rashba coupling can be tuned by an external gate electrode,[9] it is envisaged as a tool to control the precession of the electron spin in, e.g., the Datta-Das proposal for a field-effect spin transistor.[2]

2 Landauer-type formula for mesoscopic spin-polarized transport

We have recently introduced[10] an extension of standard quantum transport techniques[4,11] which allows one to study quantum interference effects in the spin-polarized transport through mesoscopic conductors containing both disorder and

different types of SO couplings, but with the spin-decoherence time[3] $T_2 \lesssim 100$ns much longer than the electron dwell time in the sample. Thus, such *mesoscopic spintronic* systems preserve both relative phases in the superpositions of spatial (i.e., orbital) quantum states that are probed in traditional mesoscopic experiments (therefore, sample size L is smaller than the dephasing length $L < L_\phi$ set by inelastic processes,[4] typically $L_\phi \lesssim 1\,\mu$m), as well as relative phases in the coherent superpositions of opposite spin states[3] of a single electron ($L < L_2 \lesssim 100\,\mu$m, where spin-decoherence length L_2 at low temperatures is determined by spin-spin interactions[3]). We also assume that spin-relaxation length L_1 characterizing the change of initial spin-polarization of injected electrons, due to processes other than Rashba+disorder effects, is smaller than L. The central result of our formalism is a direct algorithm for the *exact* computation of the zero-temperature conductance matrix[5] of a single sample

$$\mathbf{G} = \begin{pmatrix} G^{\uparrow\uparrow} & G^{\uparrow\downarrow} \\ G^{\downarrow\uparrow} & G^{\downarrow\downarrow} \end{pmatrix} = \frac{e^2}{h} \sum_{ij} \begin{pmatrix} |t_{ij,\uparrow\uparrow}|^2 & |t_{ij,\uparrow\downarrow}|^2 \\ |t_{ij,\downarrow\uparrow}|^2 & |t_{ij,\downarrow\downarrow}|^2 \end{pmatrix}, \tag{1}$$

$$\mathbf{t} = 2\sqrt{-\mathrm{Im}\,\hat{\Sigma}_L \otimes \hat{I}_\mathrm{s}} \cdot \hat{G}^r_{1N} \cdot \sqrt{-\mathrm{Im}\,\hat{\Sigma}_R \otimes \hat{I}_\mathrm{s}}, \tag{2}$$

starting from a single-particle microscopic Hamiltonian. The 2D sample is attached via perfect Ohmic contacts to two ideal semi-infinite leads, where one serves to inject spin-polarized current from ferromagnetic contacts (emitting spin-up or spin-down electrons) into a semiconductor (or nonmagnetic metal),[12] and the other one drains electrons to the contacts detecting either $\uparrow$ or $\downarrow$ electrons (the leads also define, by transverse quantization, the orbital part of an asymptotic scattering state). The partial summation in Eq. (1) adds squared amplitudes of those elements of the full transmission matrix $\mathbf{t}$ which have the same spin indices [e.g., $t_{ij,\uparrow\uparrow} = t_{2(i-1)+1,2(j-1)+1}$; $t_{ij,\uparrow\downarrow} = t_{2(i-1)+1,2j}$; $i,j = 1,...,N$]. The nonnegative matrices $-\mathrm{Im}\,\hat{\Sigma}_{L,R} = -(\hat{\Sigma}^r_{L,R} - \hat{\Sigma}^a_{L,R})/2i$ ($\hat{\Sigma}^a_{L,R} = [\hat{\Sigma}^r_{L,R}]^\dagger$) are the self-energies (r-retarded, a-advanced) describing the "interaction" of a sample with the left (L) or right (R) lead.[4,13] The $2N \times 2N$ submatrix $\hat{G}^r_{1N}$ of the full Green function matrix $\hat{G}^r_{\mathbf{nm},\sigma\sigma'} = \langle \mathbf{n},\sigma|\hat{G}^r|\mathbf{m},\sigma'\rangle$ connects the layers 1 and N along the direction of transport (x-axis). The Green function, determining the probability of phase-coherent propagation between sites $\mathbf{m}$ and $\mathbf{n}$ with or without spin-flip, is the site-spin representation of a Green operator obtained by inverting the Hamiltonian of an open system attached to the leads $\hat{G}^r = [E\hat{I}_\mathrm{o} \otimes \hat{I}_\mathrm{s} - \hat{H} - \hat{\Sigma}^r \otimes \hat{I}_\mathrm{s}]^{-1}$, where $\hat{\Sigma}^r = \hat{\Sigma}^r_L + \hat{\Sigma}^r_R$. Thus, $\mathbf{G}$ is obtained analogously to the Landauer conductance,[4] where the usual sum of the transmission probabilities over all transverse propagating modes for spinless particles $T = \mathrm{Tr}\,\mathbf{t}\mathbf{t}^\dagger$ is replaced by a 2×2 matrix of partial transmission coefficients describing the transition between left and right subsystems comprised of the two types $\uparrow, \downarrow$ of spin-polarized asymptotic states.[5] The $\mathbf{G}$-matrix allows one to compute the measured conductance in spin-resolved experiments: $\mathbf{s}^\dagger_\mathrm{i} \cdot \mathbf{G} \cdot \mathbf{s}_\mathrm{c}$, where $\mathbf{s}_\mathrm{i}$, $\mathbf{s}_\mathrm{c}$ are vectors describing the type of polarization ($\uparrow$ or $\downarrow$) of the injected and collected electrons, respectively.

In the general formalism of nonrelativistic quantum mechanics, spin degrees of freedom are internal, and are therefore described by the vectors in a spin space $\mathcal{H}_\mathrm{s}$ which is multiplied tensorially with an orbital space $\mathcal{H}_\mathrm{o}$ to get the full Hilbert space

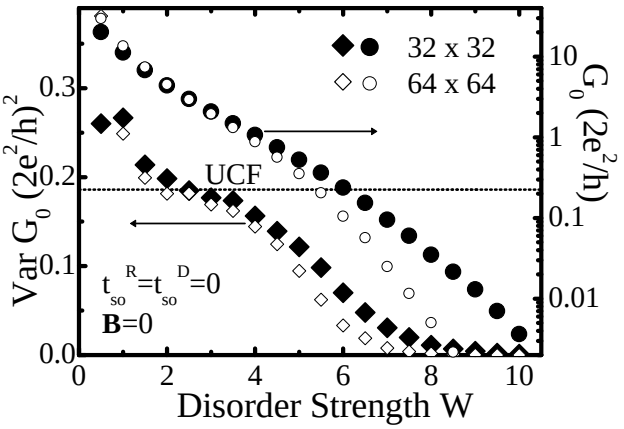

Figure 1. Conductance G_0 (circles) and its variance $\mathrm{Var}\, G_0$ (diamonds) in a quantum dot modeled on 32×32 or 64×64 half-filled tight-binding lattice as a function of disorder strength W (disorder-averaging is performed over 10000 samples). The dotted line is the value of the universal conductance fluctuations predicted perturbatively in the metallic diffusive regime.

of quantum states $\mathcal{H} = \mathcal{H}_{\rm o} \otimes \mathcal{H}_{\rm s}$. The spin-dependent interactions are accounted by the terms in a Hamiltonian that are functions of the spin operator $\hbar\hat{\boldsymbol{\sigma}}/2$ [$\hat{\boldsymbol{\sigma}} = (\hat{\sigma}_x, \hat{\sigma}_y, \hat{\sigma}_z)$ is the vector of Pauli matrices] acting in $\mathcal{H}_{\rm s}$. We choose the standard Anderson model on a square $N \times N$ lattice for the orbital part of the Hamiltonian, and cast the Rashba spin-orbit interaction in corresponding site-spin representation

$$\hat{H} = \left(\sum_{\mathbf{m}} \varepsilon_{\mathbf{m}} |\mathbf{m}\rangle\langle\mathbf{m}| + \sum_{\langle \mathbf{m},\mathbf{n} \rangle} t_{\mathbf{mn}} |\mathbf{m}\rangle\langle\mathbf{n}| \right) \otimes \hat{I}_{\rm s} + \frac{\alpha\hbar}{2a^2 t} (\hat{v}_x \otimes \hat{\sigma}_y - \hat{v}_y \otimes \hat{\sigma}_x), \quad (3)$$

where $\varepsilon_{\mathbf{m}}$ is uniformly distributed over $[-W/2, W/2]$ to simulate disorder. The single s-orbitals $|\mathbf{m}\rangle$, together with the spin eigenstates $|\sigma\rangle$ of $\hat{\boldsymbol{\sigma}} \cdot \hat{\mathbf{a}}$ ($\sigma = \uparrow, \downarrow$ is a quantum number labeling the two eigenstates, and $\hat{\mathbf{a}}$ is a unit vector along the spin-quantization axis), define a basis $|\mathbf{m}\rangle \otimes |\sigma\rangle$ in $\mathcal{H}$, and therefore a real$\otimes$spin-space representation of the operators (the local orbital basis modeling of quantum transport through nanoscopic inhomogeneous systems easily captures essential geometrical effects). Explicit use of tensor-product notation simplifies obtaining a representation of operators: for example, the velocity operator becomes a matrix $\langle\mathbf{m}|\hat{v}_x|\mathbf{n}\rangle = (i/\hbar)\, t_{\mathbf{mn}}\, (m_x - n_x)$, and $\otimes$ stands for the direct (Kronecker) product of matrices. Thus the final matrix elements in the second (Rashba) term of the Hamiltonian in Eq. (3) are just dimensionless constants multiplied by the material-specific parameters setting the energy scale $t_{\rm so}^{\rm R} = \alpha/2a$ (α is the standard parameter measuring the strength of Rashba SO interaction[6,7]).

3 Conductance fluctuations of spin-polarized electrons

A major boost for the development of mesoscopic physics came from the pioneering experimental[14] and theoretical[15] studies of unexpectedly large CF. Each quantum-

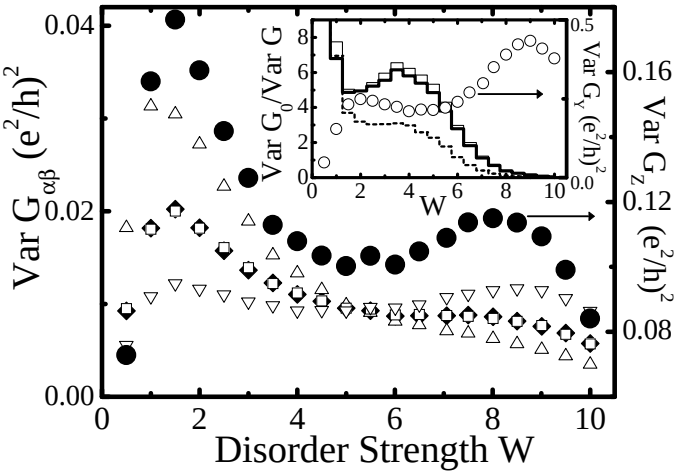

Figure 2. Zero-temperature sample-to-sample fluctuations of the components of $\mathbf{G}$ for transport which is spin-polarized $\uparrow$, $\downarrow$ along the z-axis: $\mathrm{Var}\, G^{\uparrow\uparrow}$ (diamonds), $\mathrm{Var}\, G^{\uparrow\downarrow}$ (up triangles), $\mathrm{Var}\, G^{\downarrow\downarrow}$ (squares), $\mathrm{Var}\, G^{\downarrow\uparrow}$ (down triangles), and $\mathrm{Var}\, G_Z = \mathrm{Var}\,[G^{\uparrow\uparrow}+G^{\downarrow\downarrow}+G^{\uparrow\downarrow}+G^{\downarrow\uparrow}]$ (circles), for 10000 samples modeled on a 32×32 half-filled tight-binding lattice with diagonal disorder and a strong $t_{\mathrm{so}}^{\mathrm{R}} = 1.0$ Rashba SO coupling. The inset shows: (i) the ratio $\mathrm{Var}\, G_0/\mathrm{Var}\, G$ of the fluctuations in a pure disordered case (Fig. 1) to the fluctuations of the sums of the elements of $\mathbf{G}$, where $G \equiv G_Z$ (thick solid line), G_Y (dashed line), G_X (thin solid line), for spin-polarization in the z-, y- or x-direction, respectively; (ii) peculiar features of $\mathrm{Var}\, G_Y$ (open circles) as a function of disorder strength.

coherent sample is characterized by a fingerprint of reproducible (time-independent) conductance fluctuations as a function of magnetic field, Fermi energy, or change of impurity configuration at a fixed Fermi energy. This violates the traditional notion that a given sample is well described by average values of physical quantities, particularly when $\mathrm{Var}\, G$ becomes of the same order as $\langle G \rangle$ as L approaches the localization length ξ. In diffusive ($\ell \ll L \ll \xi$) metallic ($G \gg e^2/h$) conductors, CF are considered to be universal (UCF) $\mathrm{Var}\, G = C_d (2e^2/h)^2$, so that C_d is a constant independent of the sample size or the degree of disorder[15] (C_d is reduced by a factor 2, 4, or 8 by breaking time-reversal or spin-rotation invariance, or both; for a complete list of symmetry classes and possible crossovers in weakly disordered quantum dots see Ref. 17). However, numerical studies[13] of the evolution of $\mathrm{Var}\, G$ in 3D mesoscopic metals show that CF monotonically decay with increasing disorder strength, becoming close to the constant predicted by the perturbative UCF theory[15] only in a narrow range of W. Therefore, to have a reference point for the subsequent study of fluctuations of $\mathbf{G}$, we first calculate $\mathrm{Var}\, G_0$ in the crossover between small and large W for a conductor described by the non-interacting and spin-independent Hamiltonian $\hat{H}_{\mathrm{o}}$ with $\mathbf{B} = 0 = \phi_{\mathbf{mn}}$. In this case, spin-degeneracy gives $G_0 = G^{\uparrow\uparrow} + G^{\downarrow\downarrow} = 2G^{\uparrow\uparrow}$. The result plotted in Fig. 1 demonstrates that $\mathrm{Var}\, G_0$ decreases systematically with increasing $W \in [0, 10]$, while $C_2 = 0.186$ is the expected UCF value in 2D "metals".[15]

Inspired by a recent experiment on the reduction of conductance fluctuations

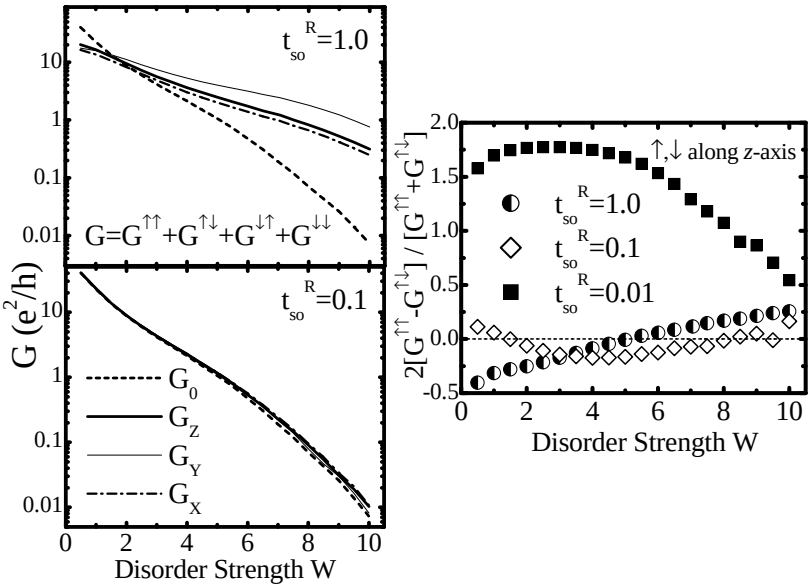

Figure 3. Total conductances (left panel) G_Z, G_Y, G_X for two different Rashba SO couplings $t_{\rm so}^{\rm R}$ (disorder-averaged over 10000 samples used also for Fig. 2). Right panel shows the relationship between $G^{\uparrow\uparrow}$ and $G^{\uparrow\downarrow}$ characterizing the propagation of spin-polarized electrons in a disordered Rashba-split systems, for both strong $t_{\rm so}^{\rm R} \sim t$ and weak $t_{\rm so}^{\rm R} \ll t$ SO coupling limit.

(CF) in open ballistic (but chaotic due to the surface scattering) quantum dots in a GaAs heterostructure in a large in-plane magnetic field,[17,16] where Rashba SO coupling was found to be essential, we undertake a similar but spin-resolved analysis for spin-polarized electrons injected into 2D disordered samples. We "create" an experiment on the computer "measuring" the components of $\mathbf{G}$ for each realization of disorder, and thereby sample-to-sample fluctuations $\mathrm{Var}\, G_{\alpha\beta} = \langle G_{\alpha\beta}^2 \rangle - \langle G_{\alpha\beta} \rangle^2$ ($\langle ... \rangle$ denotes disorder averaging) as a function of disorder strength W or Rashba coupling $t_{\rm so}^{\rm R}$. The analysis of the fluctuating properties of the components of $\mathbf{G}$, for spin-polarization $\uparrow$, $\downarrow$ in the z-direction, is shown in Fig. 2. The counterpart of the measured conductance in experiments on unpolarized electrons[17] would be to inject and collect both pure spin states, $\mathbf{s}_{\rm i} = \mathbf{s}_{\rm c} = (1 \;\; 1)^\dagger \Rightarrow G = G^{\uparrow\uparrow} + G^{\uparrow\downarrow} + G^{\downarrow\uparrow} + G^{\downarrow\downarrow}$. The fluctuating properties of G_Z, G_Y, and G_X [e.g., $G \equiv G_Z$ when the spin part, $|\uparrow\rangle$ or $|\downarrow\rangle$, of the asymptotic scattering state is an eigenstate of $\hat{\sigma}_z$, i.e., polarized along the z-axis] are analyzed (including comparison with $\mathrm{Var}\, G_0$ of Fig. 1) in Fig. 2.

4 Antilocalization in disordered Rashba-split electron system

In the quasiballistic transport regime $\ell \gtrsim L$ we find $G_0 > G_Z$, while $G_0 < G_Z$ ("antilocalization") is observed in the diffusive regime. The reduction factor $\mathrm{Var}\, G_0 / \mathrm{Var}\, G_Z$ is ≈ 5 at moderate disorder $W \simeq 2$ (where $\mathrm{Var}\, G_0 \approx C_2$), but the inset in Fig. 2 shows that it depends on the direction of magnetization of the ferromagnetic contacts, e.g., $\mathrm{Var}\, G_0 / \mathrm{Var}\, G_Y \approx 3$ around the same W. This is due

to the breaking of rotational invariance by the Rashba term (whose electric field always lies along the z-axis). The interplay of coherent scattering on impurities and spin-dependent interactions is the most pronounced when energy scale of the Rashba term in $\hat{H}$ is comparable to the strength of the disorder $t_{\rm so}^{\rm R} \simeq t$ (note that $t_{\rm so}^{\rm R}$ can be tuned, in principle, by an interface electric field[9]). Furthermore, in this limit we find that $G^{\uparrow\downarrow} > G^{\uparrow\uparrow}$ (this does not occur if the asymptotic scattering states are spin-polarized along the x- or y-axis) can hold not only in the quasiballistic regime,[5,18] but also all the way to the onset of strong localization $L \sim \xi$, as shown in Fig. 3. Moreover, Fig. 3 demonstrates that even when $t_{\rm so}^{\rm R} \ll t$ renders negligible antilocalization effects in the total conductances (i.e., G_Z, G_Y, $G_X \simeq G_0$), different components of the **G**-matrix are finite and are nontrivially related to each other in the *Rashba spin-split* ($t_{\rm so}^{\rm R} \neq 0$) electron system. We emphasize that our findings are **numerically exact**, and therefore non-perturbative in both the strength of the disorder[13] and SO interaction[2,6]—for large enough W, the mean free path $\ell \simeq 30(t/W)^2$ ceases to exist ($\ell < a \lesssim \lambda_F$) as a concept related to semiclassical transport and perturbative quantum interference effects[13] (eventually, the 2D conductor turns into Anderson insulator when[19] $L \gg \xi \simeq 1 + 5.2 \cdot 10^4/W^4$).

Acknowledgments

We thank J. Fabian, D. Frustaglia, E. I. Rashba, and I. Žutić for enlightening discussions. This work was supported in part by ONR grant N00014-99-1-0328.

References

1. S. Das Sarma *et al.*, Solid State Commun. **119**, 207 (2001).
2. S. Datta and B. Das, Appl. Phys. Lett. **56**, 665 (1990).
3. G. Burkard, H.-A. Englel, and D. Loss, Fortschr. Phys. **48**, 9-11, 965 (2000).
4. S. Datta, *Electronic Transport in Mesoscopic Systems* (Cambridge University Press, Cambridge, 1995).
5. P. Šeba *et al.*, Phys. Rev. Lett. **86**, 1598 (2001).
6. F. Mireles and G. Kirczenow, Phys. Rev. B **64**, 024426 (2001).
7. Yu. A. Bychkov and E. I. Rashba, J. Phys. C **17**, 6039 (1984).
8. S. Hikami, A.I. Larkin, and Y. Nagaoka, Prog. Theor. Phys. **63**, 707 (1980).
9. J. Nitta *et al.*, Phys. Rev. Lett. **78**, 1335 (1997).
10. B. K. Nikolić and J. K. Freericks, cond-mat/0111144.
11. C. Caroli *et al.*, J. Phys C **4**, 916 (1971).
12. M. Johnson and R.H. Silsbee, Phys. Rev. Lett. **55**, 1790 (1985).
13. B.K. Nikolić and P.B. Allen, Phys. Rev. B **63**, R020201 (2001).
14. C.P. Umbach *et al.*, Phys. Rev. B **30**, 4048 (1984).
15. B.L. Altshuler, JEPT Lett. **41**, 648 (1985); P.A. Lee, A.D. Stone, and H. Fukuyama, Phys. Rev. B **35**, 1039 (1987).
16. I.L. Aleiner and V.I. Fal'ko, Phys. Rev. Lett. **87**, 256801 (2001).
17. J.A. Folk *et al.*, Phys. Rev. Lett. **86**, 2102 (2001); B.I. Halperin *et al.*, *ibid.* **86**, 2106 (2001).
18. C.-M. Hu *et al.*, Phys. Rev. B **63**, 125333 (2001).
19. J.A. Vergés, Phys. Rev. B **57**, 870 (1998).